Remark 2.4.8 The computational work W_F of an F-cycle as introduced in Remark 2.4.4 in combination with standard coarsening is also $O(N_\ell)$ since this cycle is more expensive than the V-cycle and less expensive than the W-cycle. In particular, we obtain

$$W_F \dot{\leq} W_\ell^{\ell-1} \sum_{k=1}^{\infty} k \left(\frac{1}{4}\right)^{k-1} = W_\ell^{\ell-1} \sum_{k=1}^{\infty} \sum_{m=k}^{\infty} \left(\frac{1}{4}\right)^{m-1} = \frac{16}{9} W_\ell^{\ell-1} \tag{2.4.15}$$

and thus

$$W_F \dot{\leq} \tfrac{16}{9} C N_\ell. \qquad \gg$$

Remark 2.4.9 For 2D semicoarsening ($\tau = 2$) we find that the computational work of an F-cycle still is of the form $O(N_\ell)$. This can be seen if we take into account that a grid Ω_k is processed once more often than grid Ω_{k+1} (see Fig. 2.9). Correspondingly, if $W_\ell^{\ell-1}$ is the amount of work spent on the finest grid, then the asymptotical amount of work (for $\ell \to \infty$) of the F-cycle in case of semicoarsening is

$$W_F \dot{\leq} W_\ell^{\ell-1} \sum_{k=1}^{\infty} k \left(\frac{1}{2}\right)^{k-1} = 4 W_\ell^{\ell-1}. \qquad \gg$$

So far, we have estimated and discussed the computational work of multigrid cycles. In order to assess the numerical efficiency of such an iterative multigrid solver precisely, it is necessary to take into account both its convergence behavior and the computational effort per iteration step (cycle). For example, in order to decide how many relaxation steps $\nu = \nu_1 + \nu_2$ are appropriate per cycle and whether a V-, F- or W-cycle should be used, the effect of this decision on both the convergence speed *and* the computational work have to be analyzed. We will discuss these efficiency questions in the following section for a specific multigrid Poisson solver.

2.5 MULTIGRID CONVERGENCE AND EFFICIENCY

In this section we introduce the first specific multigrid algorithm. For that purpose we return to Model Problem 1, the discrete Poisson equation with Dirichlet boundary conditions in the 2D unit square. The algorithm presented here is a highly efficient Poisson solver. Its most characteristic multigrid component is the GS-RB relaxation for smoothing. We call it the red–black multigrid Poisson solver (RBMPS). In addition to its numerical efficiency, the algorithm is also highly parallel.

2.5.1 An Efficient 2D Multigrid Poisson Solver

The algorithm is characterized by the following multigrid components. In this characterization certain parameters and components still have to be specified:

$$- \; L_k = L_{h_k} = -\Delta_{h_k} = \frac{1}{{h_k}^2} \begin{bmatrix} & -1 & \\ -1 & 4 & -1 \\ & -1 & \end{bmatrix}_{h_k},$$

– smoother: GS-RB relaxation as presented in Section 2.1,
– restriction I_k^{k-1}: full weighting (2.3.4) (or half weighting (2.3.6), see Remark 2.5.1),
– prolongation I_{k-1}^k: bilinear interpolation (2.3.7),
– standard coarsening: $h_{k+1} = h_k/2$,
– size of coarsest grid: $h_0 = 1/2$.

Remark 2.5.1 This version of the red–black multigrid Poisson solver is a particularly simple one. There are further variants of this algorithm, some of which are even more efficient [319, 378], but less generally applicable. For example, the restriction operator FW can be replaced by HW (2.3.6) which is more efficient for certain choices of ν ($\nu \geq 3$, see Table 2.4 and Section 3.3.1). ≫

In the following we want to discuss the influence of the number of relaxations $\nu = \nu_1 + \nu_2$ and the cycle type (V, F, W) on the convergence speed of the algorithm and consequently the *numerical efficiency* of the algorithm.

We use the notation V(ν_1, ν_2), F(ν_1, ν_2) or W(ν_1, ν_2) to indicate the cycle type and the number of pre- and postsmoothing steps employed. The finest grid is $h = 1/256$. Furthermore, we can compare theoretical convergence results (which we will obtain in Chapter 3) with the measured convergence results. In Fig. 2.10 the multigrid convergence of the V(0,1)-cycle (meaning 0 pre- and 1 postsmoothing), of the V(1,1)-, the W(0,1)- and

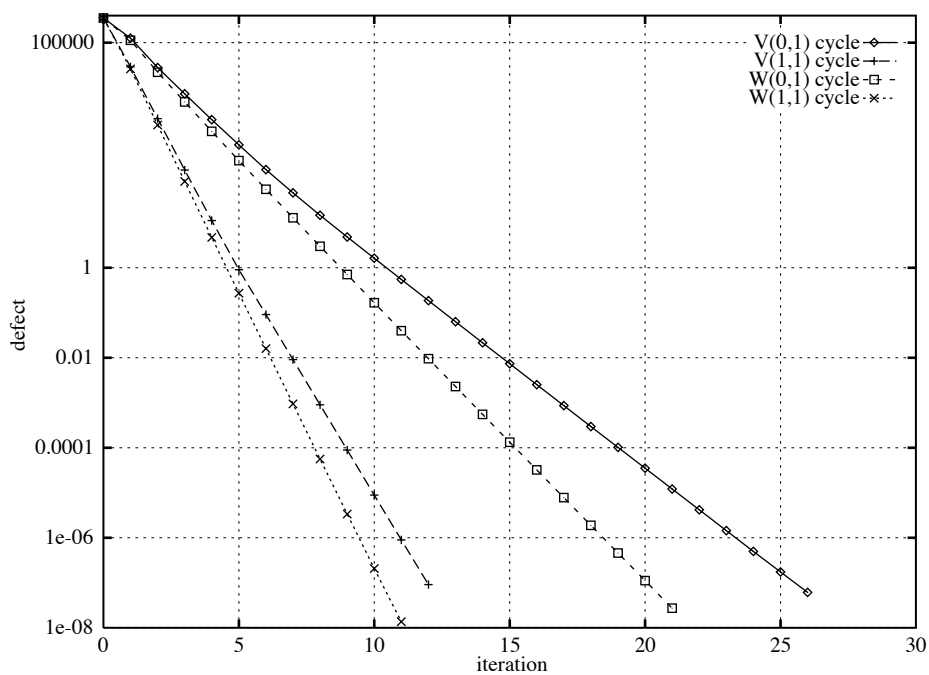

Figure 2.10. The convergence history of different RBMPS cycles for Model Problem 1.

the W(1,1)-cycle is presented, using FW as the restriction operator. The l_2 norm of the defect is plotted in a log scale along the y-axis. The x-axis shows the number of multigrid iterations. (The results obtained by the F-cycle and by the W-cycle are nearly identical.)

From Fig. 2.10, we observe rapid convergence of multigrid, especially for the V(1,1)- and W(1,1)-cycles: they reduce the defect by a factor of 10^{-12} within 12 multigrid iterations. Also the benefits of processing the coarse grid levels more frequently can be seen: the W-cycle (and the F-cycle) shows a better convergence than the V-cycle.

Remark 2.5.2 In practice, it is usually *not* necessary to reduce the defect by a factor of 10^{-12}. Convergence to discretization accuracy $O(h^2)$ (see the discussion in Section 2.6) is sufficient in most cases, and is obtained much faster. Here, we reduce the defect further in order to illustrate the *asymptotic* convergence of the multigrid cycle. ≫

2.5.2 How to Measure the Multigrid Convergence Factor in Practice

In order to construct, evaluate and analyze a multigrid iteration one often wants to determine its convergence factor ρ empirically (by measurement). In general, the only quantities that are available for the determination of ρ are the defects d_h^m $(m = 1, 2, \dots)$. We can measure, for example,

$$q^{(m)} := \frac{||\, d_h^m \,||}{||\, d_h^{m-1} \,||} \tag{2.5.1}$$

or

$$\hat{q}^{(m)} := \sqrt[m]{q^{(m)} q^{(m-1)} \dots q^{(1)}} = \sqrt[m]{\frac{||\, d_h^m \,||}{||\, d_h^0 \,||}} \tag{2.5.2}$$

in some appropriate norm, say the discrete $||\cdot||_2$ norm (see Section 1.3.3). The quantity $\hat{q}^{(m)}$ represents an average defect reduction factor over m iterations. For "sufficiently general" $d_h^0 \neq 0$ we have $\hat{q}^{(m)} \longrightarrow \rho$. $\hat{q}^{(m)}$ is a good estimate for ρ if m is sufficiently large. In many cases the *convergence history* is also of interest. This can probably be best represented by graphics as in Fig. 2.10 or by a table of the values of $q^{(m)}$.

Often the first few iteration steps do not reflect the asymptotic convergence behavior of the multigrid iteration. Then one may redefine $\hat{q}^{(m)}$ as $\hat{q}^{(m)} = \sqrt[m-m_0]{d_h^m / d_h^{m_0}}$ with a small number m_0, typically between 2 and 5.

In Table 2.2 we present the values of $q^{(m)}$ and $\hat{q}^{(m)}$ from the convergence for Model Problem 1 in Fig. 2.10 for the cycles considered.

Remark 2.5.3 When performing too many cycles, machine accuracy might limit the measurements substantially. In order to be able to perform sufficiently many iteration steps to see the asymptotic convergence behavior, it is advisable to consider the homogeneous problem ($f = 0$) with discrete solution $u_h \equiv 0$ and to start with an initial guess u^0 that is sufficiently large and general. In the case of our example, we then find asymptotic

Table 2.2. The quantities $q^{(m)}$ and $\hat{q}^{(m)}$ as a measure for the convergence of the RBMPS (with FW) for Model Problem 1 ($m_0 = 0$).

V(0,1):	$q^{(26)} = 0.343$	$\hat{q}^{(26)} = 0.333$
V(1,1):	$q^{(12)} = 0.101$	$\hat{q}^{(12)} = 0.089$
W(0,1):	$q^{(21)} = 0.243$	$\hat{q}^{(21)} = 0.238$
W(1,1):	$q^{(11)} = 0.063$	$\hat{q}^{(11)} = 0.060$

Table 2.3. Measured convergence factors of the RBMPS (with FW) for Model Problem 1 on grids of different mesh size. In each case the coarsest grid has a mesh size of $h_0 = 1/2$.

Cycle	$h = 1/512$	$h = 1/256$	$h = 1/128$	$h = 1/64$	$h = 1/32$	$h = 1/16$
V(1,1):	0.10	0.10	0.10	0.10	0.11	0.12
F(1,1):	0.063	0.063	0.063	0.063	0.063	0.067
W(1,1):	0.063	0.063	0.063	0.063	0.063	0.067

convergence factors of 0.25 for the F(0,1)- or W(0,1)-cycle and of 0.074 for the F(1,1)- or W(1,1)-cycle after a large number of multigrid iterations. ≫

***h*-independent convergence of multigrid** The numerically measured convergence of the RBMPS is essentially independent of the size of the finest grid in the multigrid cycle. This behavior is demonstrated by the results in Table 2.3. In Chapter 3, we will see that this behavior is also confirmed by multigrid theory.

2.5.3 Numerical Efficiency

In order to choose the most efficient multigrid solver, it is necessary to look at both, its convergence speed and its costs. In practice, the time needed to solve the problem is the most interesting quantity. Table 2.4 shows the wall clock times for different multigrid (cycle) iterations. The iterations stopped after the initial defects had been reduced by a factor of 10^{-12}. The times were measured on a single workstation.

Table 2.4 throws a somewhat different light on the convergence results obtained before. The V(2,1)-cycle with HW is most efficient with respect to the wall clock time on the 256^2 grid. Since W- and F-cycles have the same convergence speed for this model problem, the W-cycle clearly is less efficient than the F-cycle here.

Remark 2.5.4 Table 2.4 shows that it does not pay to use large values for ν_1 and ν_2. This is a general observation. Though the convergence factors become (somewhat) better if the number of smoothing steps is increased, it is more efficient not to smooth the error too much but rather carry out a few more multigrid cycles. In practice, common choices are $\nu = \nu_1 + \nu_2 \leq 3$. This observation can also be verified theoretically (see Section 3.3.1). ≫